



Wideband sound zone system for automotive applications

Samuel Dupont, Lucas Vindrola, Manuel Melon, Jean-Christophe Chamard,
Vincent Roussarie, Bruno Gazengel

► To cite this version:

Samuel Dupont, Lucas Vindrola, Manuel Melon, Jean-Christophe Chamard, Vincent Roussarie, et al..
Wideband sound zone system for automotive applications. 153rd Convention of the Audio Engineering
Society, Oct 2022, New York, United States. hal-03838946

HAL Id: hal-03838946

<https://hal.science/hal-03838946>

Submitted on 3 Nov 2022

HAL is a multi-disciplinary open access archive for the deposit and dissemination of scientific research documents, whether they are published or not. The documents may come from teaching and research institutions in France or abroad, or from public or private research centers.

L'archive ouverte pluridisciplinaire **HAL**, est destinée au dépôt et à la diffusion de documents scientifiques de niveau recherche, publiés ou non, émanant des établissements d'enseignement et de recherche français ou étrangers, des laboratoires publics ou privés.



Audio Engineering Society

Convention Express Paper 34

Presented at the 153rd Convention
2022 October

This Express Paper was selected on the basis of a submitted synopsis. The author is solely responsible for its presentation, and the AES takes no responsibility for the contents. This paper is available in the AES E-Library (<http://www.aes.org/e-lib>), all rights reserved. Reproduction of this paper, or any portion thereof, is not permitted without direct permission from the Journal of the Audio Engineering Society.

Wideband sound zone system for automotive applications

Samuel Dupont¹, Lucas Vindrola¹, Manuel Melon¹, Jean-Christophe Chamard², Vincent Roussarie², and Bruno Gazengel¹

¹Laboratoire d'Acoustique de l'Université du Mans (LAUM), UMR 6613, Institut d'Acoustique - Graduate School (IA-GS), CNRS, Le Mans Université, Le Mans, France

²Stellantis, Route de Gisy, 78943 Vélizy Villacoublay, France

Correspondence should be addressed to Manuel Melon (manuel.melon@univ-lemans.fr)

ABSTRACT

This paper presents and evaluates a personal sound zone system dedicated to the automotive industry. The goal is to provide a broadband system (between 100 Hz and 10 kHz) that provides a sound level contrast between different programs of at least 30 dB and a rather low reproduction error. To do this, two different speaker arrays are used: an array of eight speakers distributed on the two front headrests for the low-frequency part and arrays of 16 micro speakers for the high-frequency part (each one being located close to an ear of the two front passengers). The classical pressure matching algorithm and its weighted version are used to calculate the filters to be applied to each source. An optimisation procedure is applied to find the best set of Lagrange multipliers. Simulation results computed with point sources in a shoe-box shaped room are first used to study, analyze and optimize the array geometries. Then, measurements are performed in a semi-anechoic chamber with added wooden panels to evaluate the actual performance of the system. Finally, the results are summarized before concluding with future work directions.

1 Introduction

Personal sound zones (PSZ) have been the focus of special attention in recent decades, especially in the automotive field where the perspective of autonomous cars opens the way to new sound systems. The objective of PSZ is to deliver an audio signal to a given passenger in the car cabin while minimizing cross-talk from other passengers' programs. In the last decades, different technical solutions have been tested, from parametric arrays, to beamforming and constrained optimization of the input of distributed loudspeakers.

Among this last family and following the pioneering work of Druyvesteyn and Garas [1], several methods were developed to provide a personal listening experience. Choi *et al.* [2, 3] proposed the Acoustic Contrast Control (ACC) method which allows to control the potential energy of the pressure field in two zones:

- The Bright Zone (BZ) where the audio signal is supposed to be played;
- The Dark Zone (DZ) where the audio signal is supposed to be attenuated.

Since the ACC algorithm does not control the phase of the pressure field in the bright zone, which can lead to acoustic artifacts and unpleasant stereo images, the pressure matching (PM) method was proposed [4, 5, 6]. For this method, the deviation between the desired and the generated sound pressure field in the BZ is controlled while minimizing the acoustic potential energy in the DZ. In addition to these two principal methods, other variants have been proposed, a review of which is provided in the reference [7].

The applications of PSZ to the automotive industry are numerous in the scientific literature [8, 9, 10, 11, 12, 13]. Among other reasons, the fact that the position of the passengers is known facilitates their technical implementation. However, when the proposed solutions are based on ACC and PM algorithms, the proposed solutions have a limited frequency band. Indeed, the use of distributed loudspeaker arrays and the presence of objects whose dimensions are larger than the wavelength decrease the performance of these algorithms for frequencies above 1 or 2 kHz. In this paper, a prototype, implemented in the two headrests of car front seats, is developed. In order to cover a wide frequency band, two types of loudspeaker arrays are used:

- For the Low Frequency (LF) part (between 100 Hz and 1 kHz), eight full-band drivers (four per headrest) are implemented.
- For the High Frequency (HF) part (from 1 kHz to 10 kHz), arrays of 4 by 4 micro-speakers are used. Each of the two arrays per headrest is positioned near the ear (right or left) of a passenger.

For the two parts of the studied bandwidth, two PM methods are used to calculate the filters to apply to each speakers.

This article is organized as follows: the section 2 recalls the principles of the pressure matching algorithm and details how the crossover between the two speakers arrays is implemented. In Section 3, numerical simulations are proposed to design and validate the array geometries. The experiment set-up is then detailed in Section 4 while measurement results are presented in Section 5 for the HF array and in Section 6 for the wideband configuration. Finally, a discussion summarising the pros and cons of the proposed approach is given in Section 7.

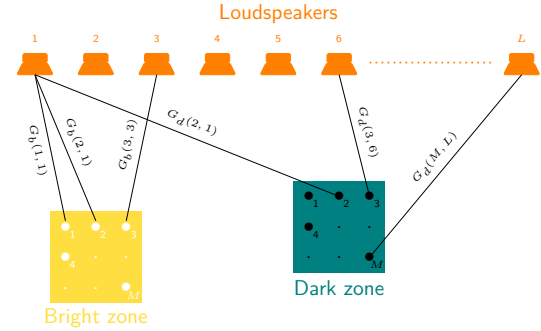


Fig. 1: Generic diagram of a sound zone system.

2 Theory

Let us begin by presenting the methods that are used to calculate the input voltages of the two speaker arrays used here. Here, we chose to test two algorithms: the classical PM method and the Weighted Pressure Matching (WPM) version [6].

Let us consider an array of L loudspeakers (with $l \in [1, L]$) as depicted in Fig. 1.

The bright and dark zones are sampled using $M = M_b + M_d$ microphones, M_b in the BZ and M_d in the DZ, (with $m \in [1, M_{b,d}]$). The transfer functions from speaker l to point m in the bright/dark zone are respectively denoted $G_b(m, l)$ and $G_d(m, l)$. To facilitate the solving of the problem, it is written in the form of vectors and matrices.

Thus, the input voltages of the speakers are denoted: $\mathbf{u} = [u_1(1), \dots, u_L(L)]$ and the pressures in the bright and dark zones are respectively given by $\mathbf{p}_b = [p_b(1), \dots, p_b(M_b)]$ and $\mathbf{p}_d = [p_d(1), \dots, p_d(M_d)]$. Matrices \mathbf{G}_b and \mathbf{G}_d are respectively given by:

$$\mathbf{G}_b = \begin{bmatrix} G_b(1,1) & \dots & G_b(1,L) \\ \vdots & G_b(m,l) & \vdots \\ G_b(M_b,1) & \dots & G_b(M_b,L) \end{bmatrix}, \quad (1)$$

and

$$\mathbf{G}_d = \begin{bmatrix} G_d(1,1) & \dots & G_d(1,L) \\ \vdots & G_d(m,l) & \vdots \\ G_d(M_d,1) & \dots & G_d(M_d,L) \end{bmatrix}. \quad (2)$$

Pressures in the bright and dark zones are then given by:

$$\begin{cases} \mathbf{p}_b = \mathbf{G}_b \mathbf{u} \\ \mathbf{p}_d = \mathbf{G}_d \mathbf{u} \end{cases} \quad (3)$$

The sound zones problem consists in determining the input voltages to applied to all speakers. This can be done using constrained optimization methods. For instance, the WPM method consists in minimizing the following cost function:

$$\mathcal{L} = (1 - \beta)(\mathbf{p}_b - \mathbf{p}_t)^H(\mathbf{p}_b - \mathbf{p}_t) + \beta(\mathbf{p}_d^H \mathbf{p}_d - \varepsilon_0) + \lambda(\mathbf{u}^H \mathbf{u} - u_0^2). \quad (4)$$

where \mathbf{p}_t is the target pressure which is chosen by the user according to the application. The β parameter allows to adjust the relative weight of the first two terms of the Lagrangian \mathcal{L} , namely the satisfaction of the target pressure and the potential energy in the dark zone. The λ parameter is used to limit the input signals of the loudspeakers in order not to damage them or to work in the linear regime. By differentiating \mathcal{L} with respect to \mathbf{u} , we get the following expression:

$$\mathbf{u} = [(1 - \beta)\mathbf{G}_b^H \mathbf{G}_b + \beta\mathbf{G}_d^H \mathbf{G}_d + \lambda\mathbf{I}]^{-1} \mathbf{G}_b^H \mathbf{p}_t. \quad (5)$$

We notice that a value of $\beta = 0.5$ allows to find the behavior of the classical PM algorithm.

Different metrics have been proposed to evaluate the performance of sound zone systems. In this paper, we use:

- The acoustic contrast AC which is given by:

$$AC = 10 \log \left(\frac{\mathbf{p}_b^H \mathbf{p}_b}{\mathbf{p}_d^H \mathbf{p}_d} \right) \text{ [dB]}. \quad (6)$$

It measures the difference in average pressure level between the BZ and the DZ. Perceptual studies [14, 15] have shown that a contrast of around 27 dB to avoid the distraction caused by an interfering program.

- The normalised mean square reproduction error Err is given by:

$$Err = \frac{(\mathbf{p}_t - \mathbf{p}_b)^H(\mathbf{p}_t - \mathbf{p}_b)}{\mathbf{p}_t^H \mathbf{p}_t} \times 100 \text{ [%]}, \quad (7)$$

and measures the error of the pressure field reproduced in the bright zone compared to the target field.

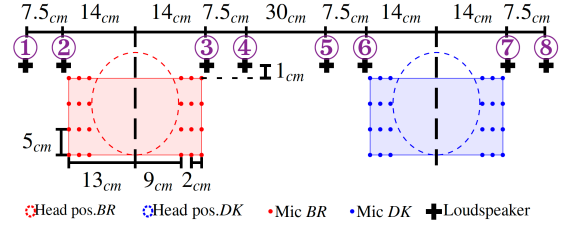


Fig. 2: Low frequency system composed by 8 sources (from Ref. [12]).

- The effort Eff ,

$$Eff = 10 \log \frac{\mathbf{u}^H \mathbf{u}}{\mathbf{u}_t^H \mathbf{u}_t} \text{ [dB]}, \quad (8)$$

is also introduced to quantify the energy that the loudspeaker array requires to satisfy the cost function \mathcal{L} relative to the energy required to produce target field only (\mathbf{u}_t being the voltage vector required to obtain the target pressure).

3 Numerical simulations

Numerical simulations in a shoe-box shaped room are first performed to help define the HF array geometry. Concerning the LF speaker array ($f < 1$ kHz), the choice was made for the geometry presented in Refs. [7, 12]. This system allowed to get a contrast AC larger than 30 dB and an error Err lower than 20%. It consists of eight speakers mounted on the headrests of the two front seats of the car (see Fig. 2).

The design of the HF part, requires first of all to choose a micro-speaker which has the desired characteristics. Thus, knowing its dimensions, it will be possible to define the geometry of the array. The micro-driver should have the following characteristics:

- small size to avoid aliasing problems when used in an array (diameter around 2 cm);
- a cut-on frequency below 1 kHz (for coupling with the LF part);
- reasonable efficiency for the size (higher than 80 dB at 50 cm);
- relatively low distortion (around 1%),
- low dispersion between units.

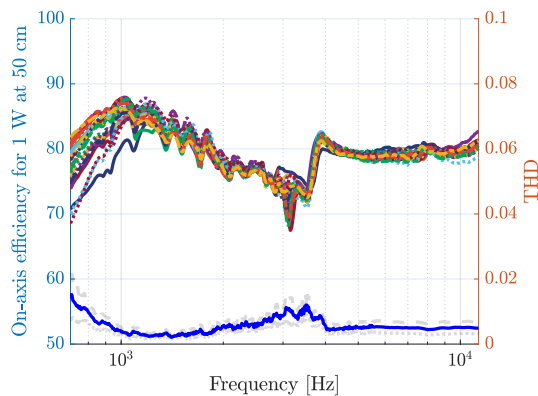


Fig. 3: On-axis efficiency for 1 W at 50 cm and distortion of 25 CMS0231KLX speakers bought at the same time.

After testing 6 candidate speakers available on the market, we chose the CMS0231KLX from CUI Devices which has a square shape with a side of 2.3 cm. The efficiency and the distortion of 25 units are represented in Fig. 3. We can see that this model fulfills most of the constraints although it exhibits a greater dispersion around its resonant frequency.

Now that the dimensions of the micro-speaker are known, it is possible to design the HF array respecting the following constraints:

- position one array per ear on each headrest, keeping room for the LF speakers;
- use small spacing between drivers to avoid aliasing problems;
- keep a reasonable number of micro-speakers per array, ideally less than 15, for future industrialization;

To meet these constraints, it was decided to use flat arrays of 4 by 4 micro-speakers (see blue dots in Fig. 4), here modeled with point sources. The dimensions of the array are 12 cm wide and 12 cm high. In the scenario presented here, the two arrays close to the driver's ears are used to play the same audio signal (mono configuration). The BZ is sampled with 2×12 microphones placed at the height of the lower speaker

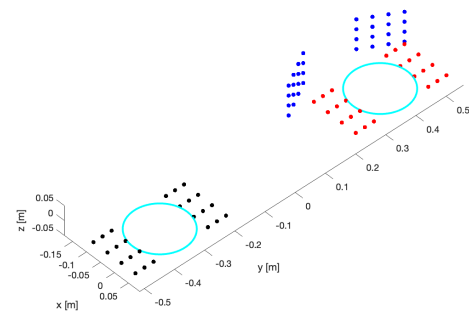


Fig. 4: Geometry of the tested scenario: the blue dots represent the HF array, the red dots represent the BZ microphone positions, while the dark navy blue dots are for the DZ microphone positions. The cyan circles represent the positions where the driver and passenger heads would be located.

(see red dots in Fig. 4). The DZ is also split into two parts, one for each ear of the driver (see dark navy dots in Fig. 4).

This set-up has been tested in a rectangular room of dimensions $2 \text{ m} \times 1.4 \text{ m} \times 1.5 \text{ m}$ modelled using a image source method with a maximum source order of 5. The absorption coefficient of the walls is homogeneous and was chosen to represent the average acoustic behavior of a car cabin (see Fig. 5).

The target pressure p_t is calculated in the bright zone with all speaker driven with the same input signal. The following procedure has been used to determine the best set of β and λ parameters: their values are chosen as being those which maximize the contrast while keeping an effort lower than 8 dB (in order to spare the

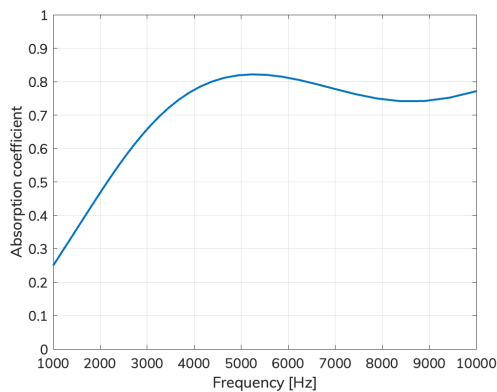


Fig. 5: Absorption coefficient of the walls of the rectangular room.

micro-speakers) and an error lower than 20% (in order to maintain a good playback quality). To illustrate this method, surface plots of the contrast as a function of β and λ are given in Fig. 6 with a color scale giving the effort Eff and Fig. 7 with a color scale giving the effort Err . On both Figures, the red marker allows to show the chosen β and λ values. While the effect of λ is quite monotonous over a large range of values, we notice that the effect of the β parameter is very sharp with a sudden increase of the contrast when it approaches a unity value. It is indeed difficult for such a small array to provide both a good contrast and a low reproduction error, with respect of the phase, in the BZ. The values of λ close to one provided by the optimization procedure give a behavior similar to that of an "Acoustic Contrast Control" (ACC) algorithm with however a constraint on the phase somehow preserved ($Err < 20\%$) but more relaxed than for the classical PM algorithm (with $\beta = 0.5$).

The results of the metrics obtained for this simulation are shown in Fig. 8. We observe that above 1200 Hz, the contrast AC is superior to the 30 dB target. Between 1 and 2 kHz, AC oscillates between 25 and 35 dB. Adding additional speakers or increasing the size of the array would increase AC , which however is not compatible with a headrest implementation. We also notice in Fig. 8, that the contrast is well bounded at 8 dB and the error at 20%, in accordance with what was set during the optimization of λ and β . It is now time to experiment with this design in a real situation.

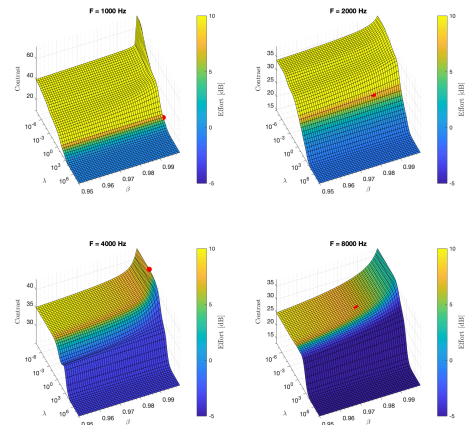


Fig. 6: Maps of the WPM contrast for four frequencies as function of the λ and β parameters. The color scale indicates the effort Eff . The red marker indicates β and λ values that maximizes the contrast by limiting the effort to a maximum of 8 dB and the error to a maximum of 20%.

4 Experimental setup

Two headrest prototypes have been built. Each one includes 4 Tectonic TEBM35C10-4 speakers and are separated by the distance shown in Fig. 2. Only the driver's headrest is equipped with two arrays of 4 by 4 CUI CMS0231KLX drivers (one for each ear). The HF arrays are shown in Fig. 10 as well as the microphones sampling the BZ. The mesh of the BZ and DZ is the same as for the numerical simulation. Here, each microphone line, composed of 4 Brüel & Kjaer 4958 microphones, is moved between each measurement to form the BZ and DZ grids. Because of the presence of the HF arrays, the two Tectonic drivers in the center of the driver's headrest are lowered by 5 cm in respect to the line passing through the other six Tectonic drivers.

The headrests are then mounted on two car front seats in which two artificial heads are also positioned (see Fig. 9). The entire system is then installed in a semi-anechoic chamber. Note that a wooden panel has been added on the left and right sides to add some reflections and complicate the acoustic environment.

The forty loudspeakers are then connected to ten four-

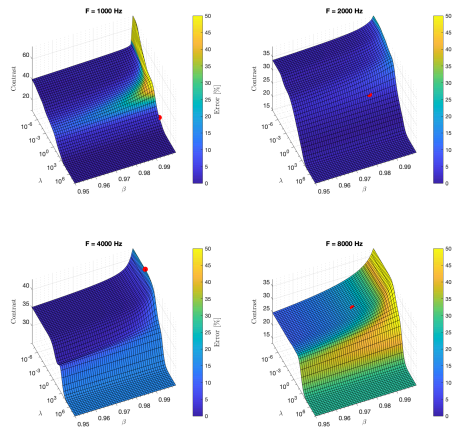


Fig. 7: Maps of the WPM contrast for four frequencies as function of the λ and β parameters. The color scale indicates the error Err . The red marker indicates the β and λ values that maximizes the contrast by limiting the effort to a maximum of 8 dB and the error to a maximum of 20%.

channel amplifiers of type HPA D604. Finally, a MAD-Iface XT audio interface is used to drive two RME M-32 DA digital-to-analog converters for the speakers and one RME M-16 AD digital-to-analog converter for the microphones. Exponential sine sweep signals have been used for all measurements.

5 Experimental results: HF array

Once the measured versions of the \mathbf{G}_b and \mathbf{G}_d matrices have been obtained, they are used to compute the performance metrics. Here, only the driver's left and right ears array are used for both the target pressure definition and for the HF transfer function measurement. Fig. 11 shows the acoustic contrast AC , the error Err and the Effort Eff for the HF array between 1 and 9 kHz. In this semi-anechoic configuration, the WPM contrast is rather good with values between 30 and 48 dB in the studied frequency range: 1 kHz to 9 kHz. We can also see that the contrast obtained for WPM is 5 to 10 dB higher than the one obtained by the PM method. We also notice that the effort is effectively limited to 8 dB and the error to 20%.

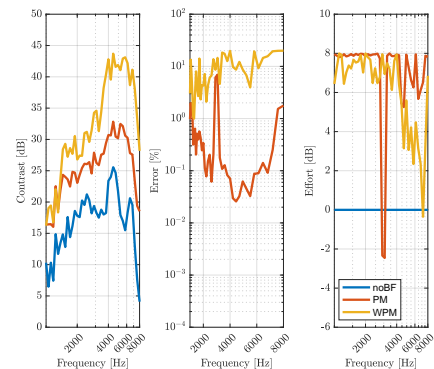


Fig. 8: Frequency response of the contrast, the error and effort of the simulated case. Blue: no processing, red: classical PM ($\beta = 0.5$ and λ optimised), yellow: WPM (β and λ optimised).



Fig. 9: Experimental set-up.

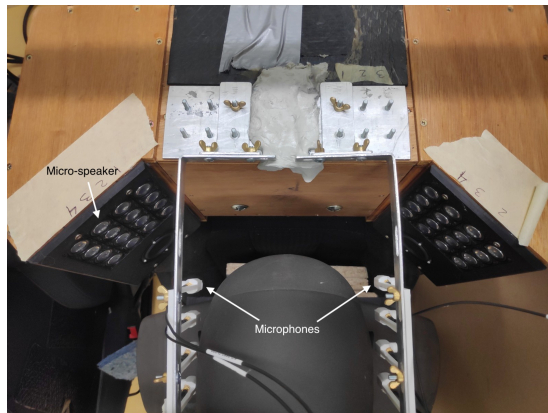


Fig. 10: Picture of the HF array.

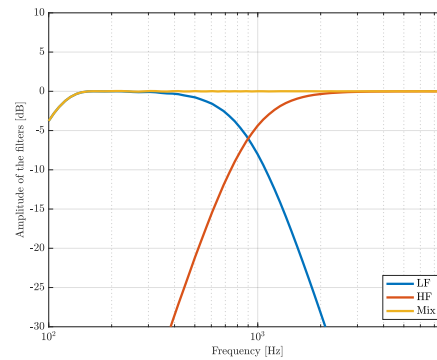


Fig. 12: Frequency response of the array crossover filters: Blue: LF array filter, red HF array filter, yellow sum of the filters.

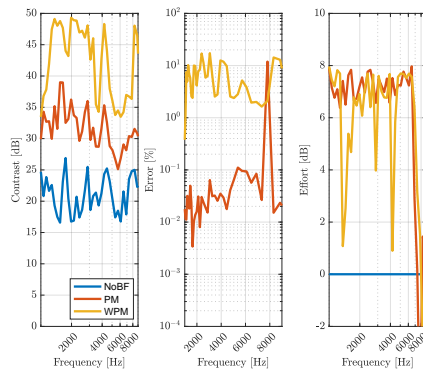


Fig. 11: Frequency response of the contrast, the error and effort of the semi-anechoic case. Blue: no processing, red: classical PM ($\beta = 0.5$ and λ optimised), yellow: WPM (β and λ optimised).

6 Experimental results: wideband system

The next step is to experimentally test the wideband system. In order to combine the responses of the two loudspeaker arrays, crossover FIR filters are used:

- A band-pass filter between 70 Hz and 900 Hz for the LP array of order 2;
- A high-pass filter of order 2 with a cut-off frequency of 900 Hz for the high frequency array.

The crossover filters are then applied to the LF and HF arrays to build the wideband system. The contrast has been measured using two scenarios:

- An offline mode for which the contrast is calculated using measured \mathbf{G}_b and \mathbf{G}_d .

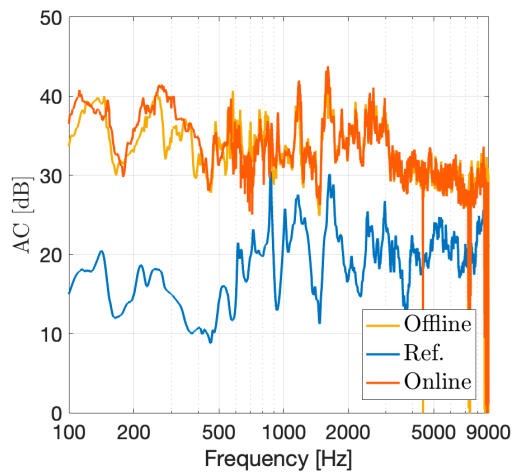


Fig. 13: Contrast for the PM method. Yellow: offline, orange: Online, blue: no filter.

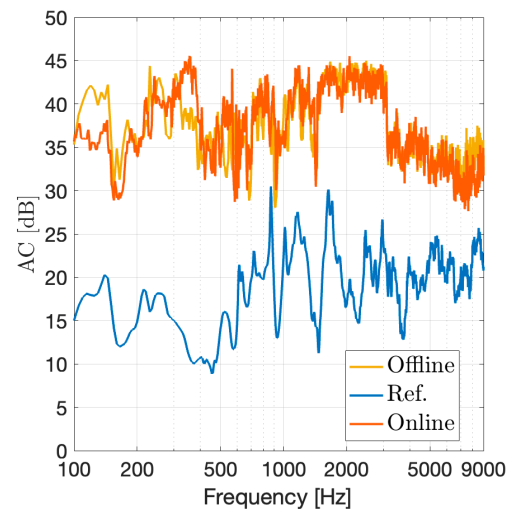


Fig. 14: Contrast for the WPM method. Yellow: offline, orange: Online, blue: no filter.

- An online mode, for which PSZ filters are first computed for all frequencies, and then their impulse responses are obtained using an inverse Fourier transform. Afterwards, the PSZ and crossover filters are applied to logarithmic swept sinusoidal signals. Finally, the filtered signals are played through the speaker arrays and recorded in the BZ and DZ to calculate the actual contrast.

The obtained contrast curves are plotted in Fig. 13 for PM and in Fig. 14 for WPM. Firstly we notice that in both cases the online and offline results are quite close, with more marked differences in low frequencies which can be attributed to the background noise due to the ventilation of the measurement room. The WPM algorithm provides a better contrast than the PM algorithm, but this gain is most noticeable in the 1 to 4 kHz band.

7 Discussion

In this paper, a broadband system for personal sound zones in the automotive context has been tested. The implementation of this system is done in the headrests. It consists of a distributed array of loudspeakers as proposed in Ref. [7] for the low frequency part. In the high frequency range, a compact array of micro-speakers has been proposed. It consists of two square arrays of

16 speakers per headrest, each array being placed close to each ear.

Two pressure matching algorithms (classical and weighted version) were first tested on the HF part and allowed to achieve a high contrast by limiting the effort to 8 dB allowing the reproduction error to be raised to a maximum of 20%.

Then, the broadband system was implemented using crossover filters. The obtained contrast, evaluated in online and offline mode, is also higher than 30 dB on almost all the 100 Hz–9 kHz band.

To confirm these first results, the following complementary studies could be carried out. First of all, the system should be tested in a real car cabin to check if the contrast is maintained above 30 dB. Based on reference [13], a study of the robustness of the PSZ filters to changes in the environment (movement of heads, seats, change in temperature, etc.) could be performed. Indeed, due to the shorter wavelengths, the influence of these changes in HF should be more important than in LF and the use of adaptive PSZ filters should be even more relevant than in low frequencies. Finally, the effect of the non-linearities of the micro-speakers could also be investigated.

References

- [1] Druyvesteyn, W. and Garas, J., “Personal sound,” *J. Audio Eng. Soc.*, 45(9), pp. 685–701, 1997.
- [2] Choi, J. and Kim, Y.-H., “Generation of an acoustically bright zone with an illuminated region using multiple sources,” *J. Acoust. Soc. Am.*, 111(4), pp. 1695–700, 2002.
- [3] Elliott, S. J., Cheer, J., Choi, J.-W., and Kim, Y., “Robustness and Regularization of Personal Audio Systems,” *IEEE Trans. on Audio, Speech, Language Process.*, 20(7), pp. 2123–2133, 2012.
- [4] Poletti, M., “An investigation of 2-d multizone surround sound systems,” in *Audio Engineering Society Convention 125*, 2008.
- [5] Chang, J.-H. and Jacobsen, F., “Sound field control with a circular double-layer array of loudspeakers,” *J. Acoust. Soc. Am.*, 131(6), pp. 4518–4525, 2012.
- [6] Olivieri, F., Fazi, F., Nelson, P., and Fontana, S., “Comparison of strategies for accurate reproduction of a target signal with compact arrays of loudspeakers for the generation of zones of private sound and silence,” *journal of the audio engineering society*, 64(11), pp. 905–917, 2016.
- [7] Vindrola, L., *Personalised low-frequency sound reproduction in a car cabin*, Ph.D. thesis, Le Mans University, 2021.
- [8] Cheer, J., *Active control of the acoustic environment in an automobile cabin*, Ph.D. thesis, University of Southampton, 2012.
- [9] Liao, X., Cheer, J., Elliott, S. J., and Zheng, S., “design of a loudspeaker array for personal audio in a car cabin,” *J. Audio Eng. Soc.*, 65(3), pp. 226–238, 2017.
- [10] Widmark, S., *Causal MMSE Filters for Personal Audio : A Polynomial Matrix Approach*, Ph.D. thesis, Uppsala University, 2018.
- [11] Møller, M. and Olsen, M., “On in situ beamforming in an automotive cabin using a planar loudspeaker array,” in *Proceedings of the ICA 2019 and EAA Euroregio*, pp. 1109–1116, 2019.
- [12] Vindrola, L., Melon, M., Chamard, J.-C., and Gazengel, B., “Pressure Matching With Forced Filters for Personal Sound Zones Application,” *J. Audio Eng. Soc.*, 68(11), pp. 832–842, 2020.
- [13] Vindrola, L., Melon, M., Chamard, J.-C., and Gazengel, B., “Use of the filtered-x least-mean-squares algorithm to adapt personal sound zones in a car cabin,” *J. Acoust. Soc. Am.*, 150(3), pp. 1779–1793, 2021.
- [14] Francombe, J., Mason, R., Dewhurst, M., and Bech, S., “Elicitation of attributes for the evaluation of audio-on-audio interference,” *The Journal of the Acoustical Society of America*, 136(5), pp. 2630–2641, 2014.
- [15] Baykaner, K. R., *Predicting the Perceptual Acceptability of Auditory Interference for the Optimisation of Sound Zones.*, Ph.D. thesis, University of Surrey, Guildford, 2014.